Lou et al., http://www.jcb.org/cgi/content/full/jcb.201409001/DC1

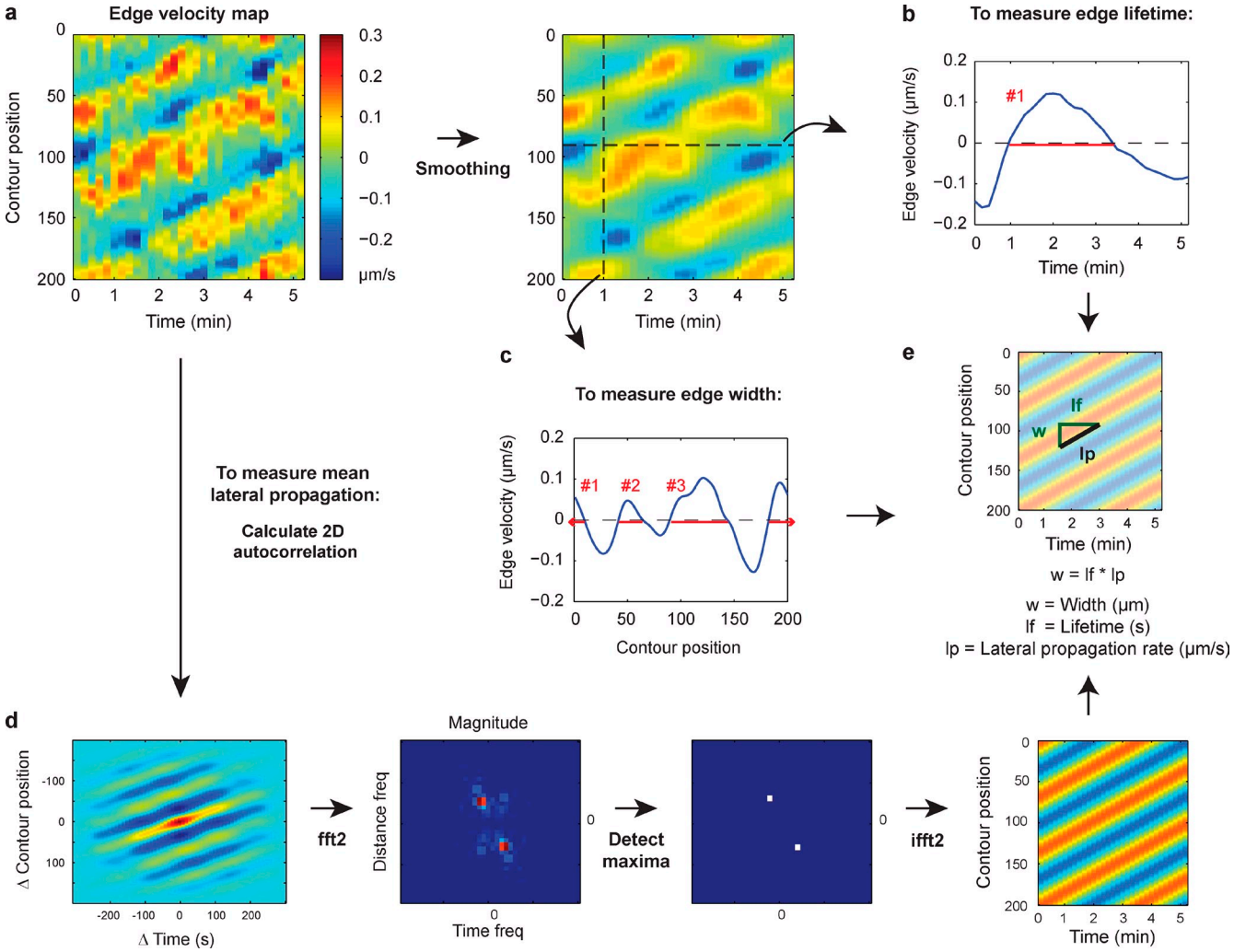

Figure S1. **Diagram of how edge width, edge lifetime, and lateral propagation measurements are made.** (a) To measure edge width, lifetime, and lateral propagation rate from edge velocity maps, we first applied a Gaussian filter with an SD of three contour points and 20 s to make measurements more reliable. (b) To measure edge lifetime, we took temporal slices through the edge velocity map at every contour point and identified regions where the edge velocity was >0. The width of those regions was recorded in seconds as the edge lifetime. To further reduce measurement variability, we recorded the mean of all edge lifetimes identified for each cell. (c) To measure edge width, we took contour slices through the edge velocity map at every moment in time and identified regions where the edge velocity was >0. The width of those regions was recorded in contour point units and then converted to microns. To reduce measurement variability, we recorded the mean of all edge widths identified for each cell. (d) To measure the mean lateral propagation rate, we calculated the 2D autocorrelation of the edge velocity map to highlight dominant frequencies. We then applied the 2D Fourier transform and identified all frequencies having amplitudes of at least half of the maximum. We fit Gaussians to the identified maxima to achieve subpixel resolution for frequency identification. Each lateral propagation frequency in the edge velocity map gives rise to two maxima in Fourier space. We then converted the frequency information to micrometers/second units. Shown on the right is the reconstruction of the lateral propagation pattern using only the frequency information encoded in the detected maxima. It faithfully recapitulates the actual pattern found in the input. Note that we discarded the phasing information for the reconstruction shown here. (e) Given that 4-dpf cells have multiple protrusions that travel laterally around the cell, the properties of edge width, edge lifetime, and lateral propagation rate are inextricably linked in the steady-state, as shown in the diagram.

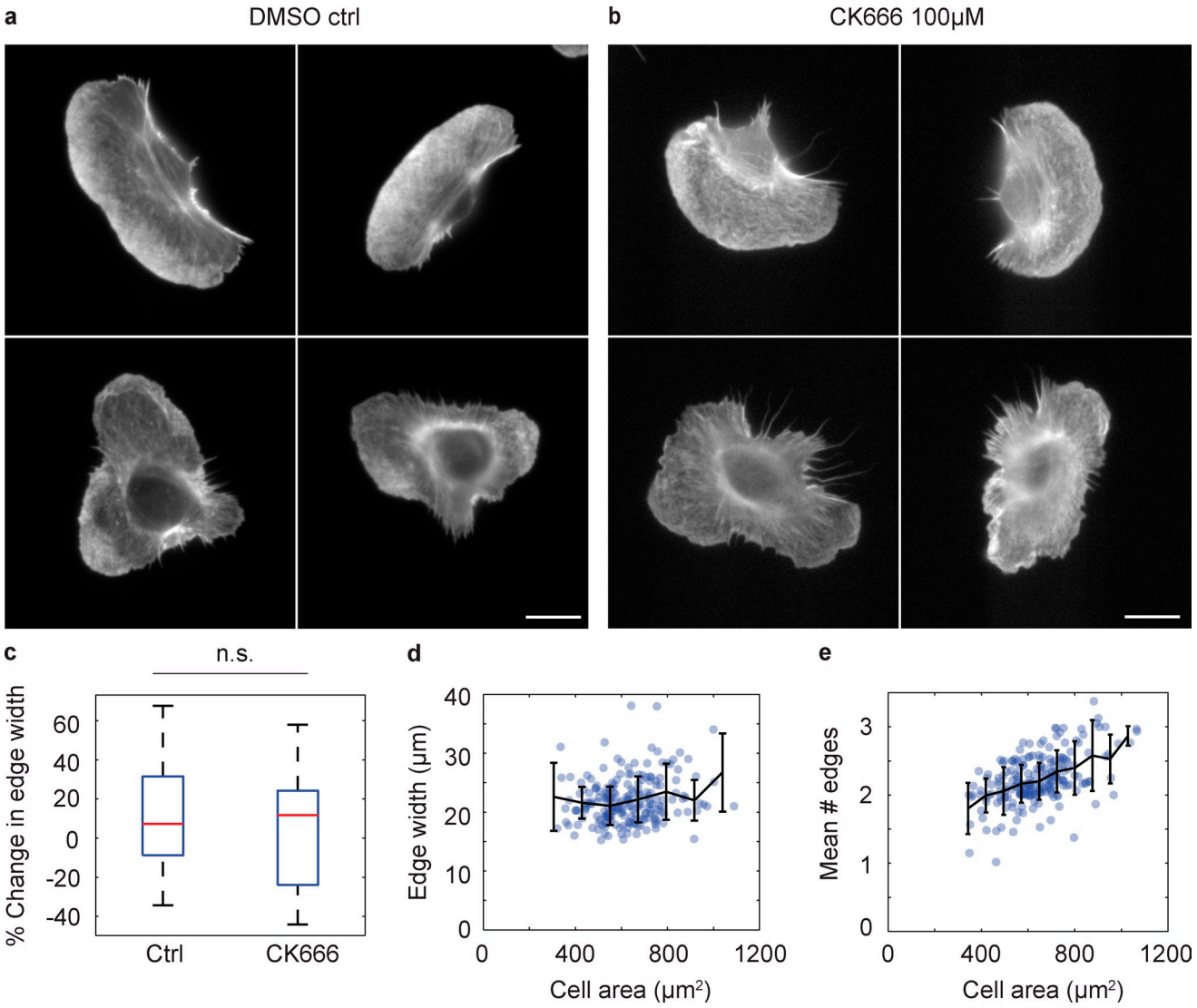

Figure S2. **The branching/capping ratio and cell size do not regulate edge width.** (a and b) Phalloidin staining of 4-dpf cells treated with either DMSO control (a) or 100 µM CK666 (b) for 15 min. Bars, 10 µm. (c) Protrusion width measured in individual 4-dpf multiple-front cells before and after addition of DMSO control (n = 14) or 100 µM CK666 (n = 14). Percentage change in edge width after drug treatment is shown. $P > 0.05$ as measured by two-sample t test. (d) Mean protrusion width and mean cell area measured for individual 4-dpf multiple-front cells (n = 209). Error bars indicate SD. (e) Mean number of protrusions and mean cell area observed in individual 4-dpf multiple-front cells over 10 min (n = 211).

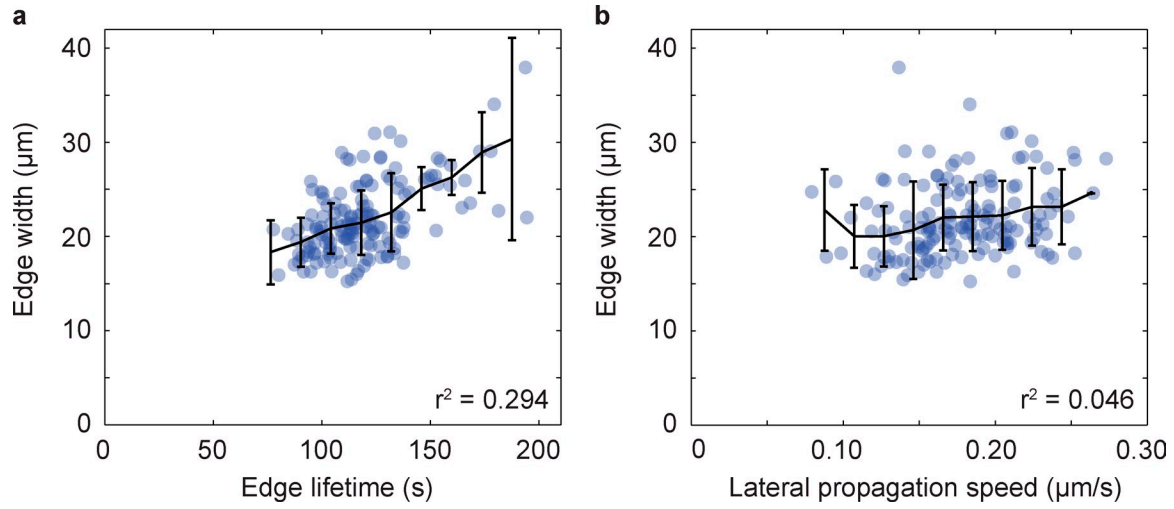

Figure S3. **Edge width is correlated with edge lifetime and the lateral propagation rate.** (a) Edge width is correlated with edge lifetime. Each dot represents mean width and lifetime measured in an individual cell (n = 154). Error bars indicate SD. (b) Edge width is weakly correlated with lateral propagation speed. Each dot represents mean width and the lateral propagation rate measured in an individual cell (n = 154). Error bars indicate SD.

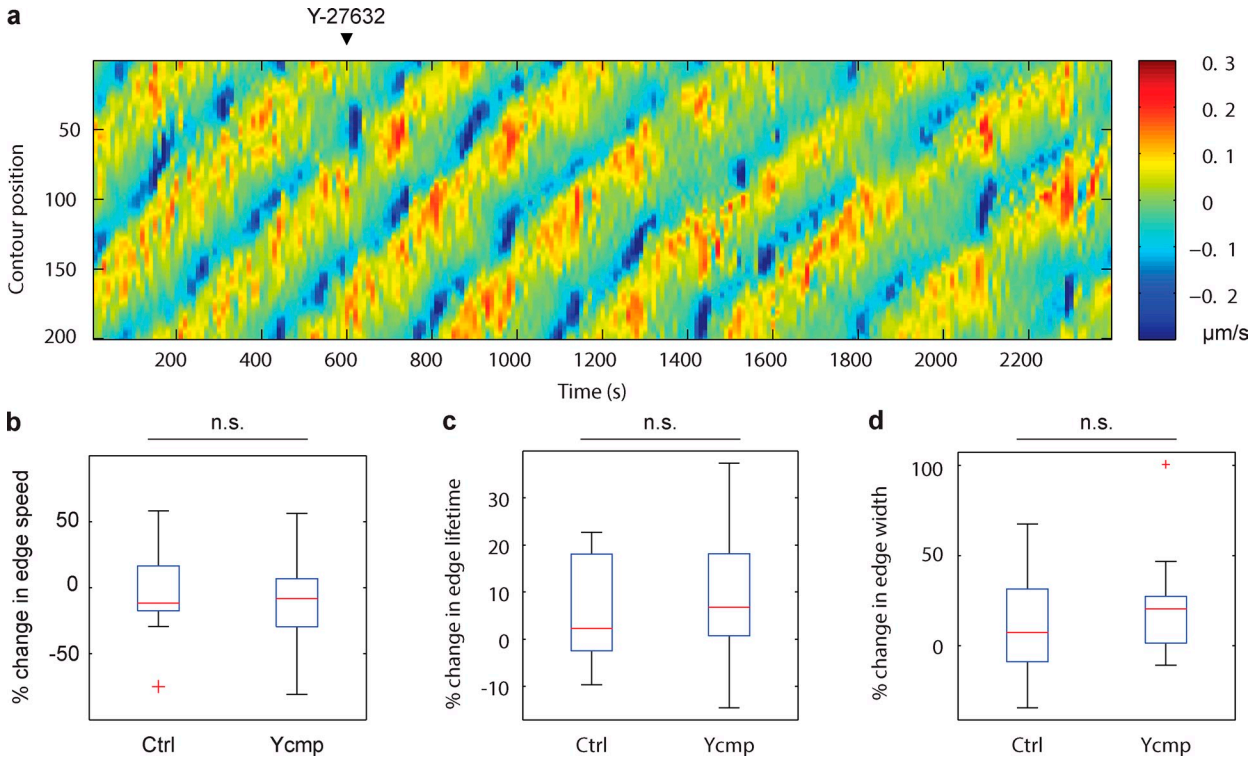

Figure S4. **Y-27632 has no effect in zebrafish keratocytes.** (a) Example edge velocity map for a cell treated with 100 μM Y-27632. (b–d) Percentage change in protrusion speed (b), lifetime (c), and width (d) measured in individual cells before and after treatment with either a DMSO control (n = 14) or Y-27632 (n = 15). Data are pooled across cells treated with 30 μM, 100 μM, and 300 μM of drug. No effect was observable even at a 300-μM concentration. n.s., $P > 0.05$ as measured by a two-sample t test.

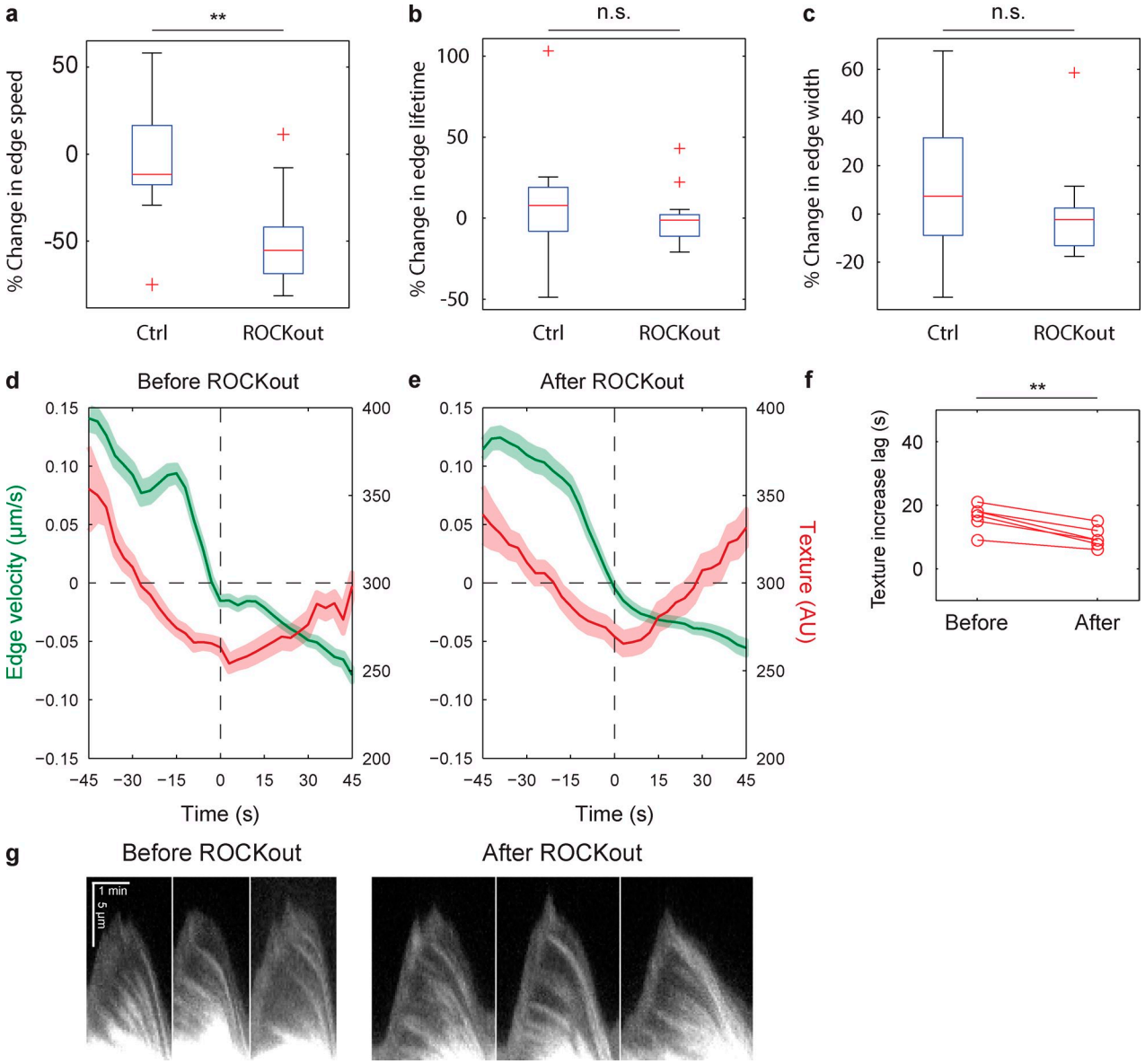

Figure S5. **ROCKout does not influence edge lifetime or width.** (a–c) Percentage change in protrusion velocity (a), lifetime (b), and width (c) measured in individual cells before and after treatment with either DMSO control (n = 14) or 50 µM ROCKout (n = 14). (d and e) Myosin accumulation behind the leading edge over time quantified in the representative cell shown in Fig. 7 c using an image texture score (see Materials and methods) before (d) and 2–5 min after (e) addition of 50 µM ROCKout. (f) Time lag between retraction onset and onset of myosin texture increase as measured in 4-dpf cells before and after addition of 50 µM ROCKout (n = 6). (g) Example kymographs taken from the cell shown in Fig. 7 c. **, $P < 0.01$; n.s., $P > 0.05$ as measured by a two-sample t test.

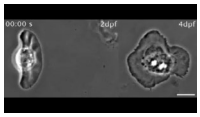

Video 1. **Zebrafish keratocytes behave differently depending on the developmental stage.** Time-lapse phase microscopy movie of representative 2-dpf (left) and 4-dpf multiple-front keratocytes (right). Images were acquired with a wide-field microscope (Ti Eclipse; Nikon). The time stamp (top left) is in the format minutes:seconds. Frames were acquired every 20 s for 3 min and are displayed at 5 frames per second. Bar, 10 µm. This video corresponds to Fig. 1 a.

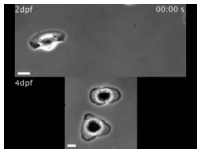

Video 2. **4-dpf cell protrusions remain small after DMSO treatment and washout.** Time-lapse phase microscopy movie of a representative 2-dpf (top) and 4-dpf (bottom) keratocyte before, during, and after 10% DMSO treatment. Addition of DMSO is indicated with red text (bottom right). Images were acquired with a wide-field microscope (Ti Eclipse; Nikon). The time stamp (top right) is in the format of minutes:seconds. Frames were acquired every 20 s for 20 min and are displayed at 5 frames per second. Bars, 10 µm. This video corresponds to Fig. 3 b.

Video 3. **ML7 converts multiple-front 4-dpf cells to the single-front phenotype.** Time-lapse epifluorescence microscopy movie of a 4-dpf keratocyte expressing EGFP-CAAX before and after addition of 25 µM ML7. ML7 addition is indicated with red text (top right). Images were acquired with a wide-field microscope (Ti Eclipse; Nikon). The time stamp is in the format of minutes: seconds before/after ML7 addition (top left). Frames were acquired every 10 s for 34 min and are displayed at 15 frames per second. Bar, 10 µm. This video corresponds to Fig. 5 a.

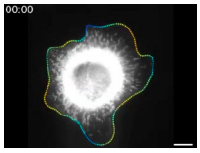

Video 4. **Myosin localization in a multiple-front 4-dpf cell.** Time-lapse epifluorescence microscopy movie of a 4-dpf keratocyte expressing mApple-tagged myosin light chain. Cell edge position is indicated by the colored dots, where color represents edge velocity: red is protruding, blue is retracting, according to the color bar in Fig. 6 a. Images were acquired with a wide-field microscope (Ti Eclipse; Nikon). The time stamp is in the format minutes:seconds (top left). Frames were acquired every 3 s for 4 min and are displayed at 20 frames per second. Bar, 10 µm. This video corresponds to Fig. 6 a.

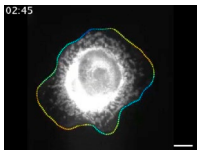

Video 5. **Myosin localization in a multiple-front 4-dpf cell after ML7 treatment.** Time-lapse epifluorescence microscopy movie of the same cell as in Video 4, expressing mApple-tagged myosin light chain. Cell edge position is indicated by the colored dots, where color represents edge velocity: red is protruding, blue is retracting, according to the color bar in Fig. 6 a. Images were acquired with a wide-field microscope (Ti Eclipse; Nikon). The time stamp is in the format minutes:seconds after ML7 addition (top left). Frames were acquired every 3 s for 5 min and are displayed at 20 frames per second. Bar, 10 µm. This video corresponds to Fig. 6 b.

Supplemental file 1, Calculate_edge_properties.m, contains the code to measure protrusion width, velocity, lifetime, and lateral propagation rate given an edge velocity matrix, as described in Fig. S1.